Use of radar measured rainfall for hydrologic modelling

G.S. SCHELL[1], C.A. MADRAMOOTOO[2], G.L. AUSTIN[3], and R.S. BROUGHTON[2]

[1]Ecological Services for Planning Ltd., 361 Southgate Drive, Guelph, ON, Canada N1G 3M5; [2]Department of Agricultural Engineering, Macdonald College of McGill University, 21111 Lakeshore Road, Ste. Anne de Bellevue, PQ, Canada H9X 1C0; and [3]Former Director, McGill Weather Radar Observatory, Ste. Anne de Bellevue, PQ, Canada H9X 1C0. *Received 13 February 1990; accepted 20 June 1991.*

Schell, G.S., Madramootoo, C.A., Austin, G.L. and Broughton, R.S. 1992. **Use of radar measured rainfall for hydrologic modelling**. Can. Agric. Eng. **34**:041-048. The capability of radar measured rainfall to enhance the simulation of storm hydrographs was assessed. Six rainfall events occurring in 1986 and 1987 over an 8.13 km^2 agricultural watershed in south-western Quebec were measured by the McGill weather radar, and input to the hydrologic model, HYMO. The model utilized the SCS curve number method to generate surface runoff. Simulated streamflow hydrographs were compared with observed storm flows. For short duration, high intensity, spatially variable rainfall events, there were minor improvements in hydrograph simulations when calibrated radar measured rainfalls were input to the model, compared to tipping-bucket raingauge measurements. Prolonged, low intensity storms were poorly simulated by the model using either rainfall data source.

La capacité des mesures pluviométriques obtenues à l'aide du radar d'améliorer la simulation des hydrogrammes a été évaluée. Six événements de pluie qui eurent lieu en 1986 et 1987 sur un bassin versant agricole de 8.13 km^2 du sud ouest du Québec, ont été mesurés par le radar de McGill, et ont été entrés dans le modèle hydrologique HYMO. Le modèle utilisait la méthode du numero de courbe (SCS Curve Number) pour générer le ruissilement de surface. Les hydrogrammes obtenus par simulation ont été comparés aux écoulements observés. Pour les pluies de courte durée, de haute intensité, spatialement distribuées, il y a eu des améliorations mineures des résultats de simulation lorsque les mesures pluviométriques du radar ont été entrées dans le modèle au lieu des mesures obtenues par le pluviomètre.Les tempêtes de longue durée et de faible intensité ont été simulées assez mal par le modèle, peu importe la source de données utilisée.

INTRODUCTION

Most rainfall-runoff modelling studies on agricultural watersheds are limited to using data that are inexpensively obtained and readily available. A single tipping-bucket raingauge is generally used to obtain rainfall inputs for hydrologic models, for economic and logistical reasons. However, many rainfall events, particularly summer convective storms, exhibit considerable spatial variability. One or two point measurements by raingauges may be inadequate. The success of the modelling exercise may be compromised by rainfall inputs that are not representative of the amount of rainfall over the entire modelled catchment. One solution to this problem is to use rainfall measurements from a weather radar, calibrated with data from a raingauge located near the study area.

Radar can provide measurements of rainfall intensity every five or ten minutes, over an array of areas of 1 km^2 or less. Depending on the radar installation, rainfall data may be available in real-time, i.e. within a few minutes of when they are received by the radar, or from an archived data base of historical storm events. Both forms of rainfall data can be used in a wide range of hydrologic modelling applications.

The use of rainfall measurements from a radar can be a practical alternative to installing and maintaining a network of raingauges in regions where rainfall data from a weather radar or radar archives are available. There is a need to demonstrate and evaluate the benefits of using radar measured rainfall for input to hydrologic models.

The purpose of this study was to investigate the feasibility of using the McGill weather radar, located at Ste. Anne de Bellevue, PQ, to generate rainfall input data for the hydrologic model, HYMO, for a small rural watershed. Simulated outputs were compared with those obtained using measurements from a single raingauge, and with observed streamflows.

STUDY AREA

Site

The study watershed, 8.13 km^2 in area, is located approximately 20 km to the south-west of the McGill radar, at St. Dominique, PQ (Fig. 1). The watershed is primarily agricultural.

A main watercourse, 5.2 km in length, flows from the north to the south end of the watershed. A smaller channel joins the main watercourse 0.9 km upstream from the channel stage recorder. The average basin slope is 0.19%. During the summer and early autumn, heavy weed growth in both channels causes a reduction in channel flow velocity.

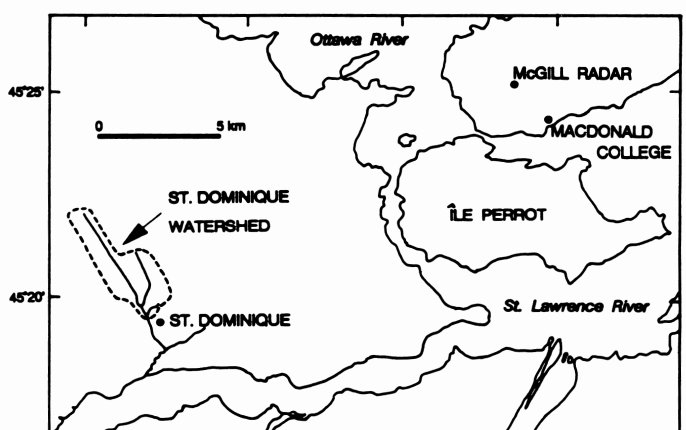

Fig. 1. Location map of the St. Dominique watershed.

Soils and land-use

Soils data and information about cropping patterns and vegetation are summarized in Table I.

Throughout most of the catchment the predominant soil type is a sandy loam, 0.3 to 0.8 m thick, overlying a clay subsoil. A small section of loamy fine sand occurs in the northern part of the watershed, and a clay soil predominates in the south east portion.

Table I. Soil and land-use characteristics of the St. Dominique watershed (after Enright and Madramootoo 1988)

Soil Type	% of watershed area	Cropping Pattern	% of watershed area
Clay	21	Corn	24
Loamy fine sand	9	Hay/pasture	22
Muck	3	Lawn sod	14
Sandy loam	67	Tree nursery	14
		Vegetables	4
		Woods	22

Approximately 31% of the watershed is subsurface drained, primarily in the southern end (Madramootoo et al. 1988). A network of drainage ditches has been established alongside most roads and through many fields in the catchment basin.

Instrumentation

A tipping-bucket recording raingauge was installed near the lower section of the watershed.

A water level recorder was installed in the main channel at the basin outlet. A rating curve was developed at this location using a velocity meter during rising and falling water levels, and channel cross-section measurements. Streamflow hydrographs were produced by collating stream depth from the water level recorder charts with the rating curve.

HYDROMETEORLOGICAL DATABASE

Six rainfall events occurring between July 1986 and October 1987 were selected for analysis. Some characteristics of the storms are listed in Table II, along with the observed baseflow and peak flowrates at the St. Dominique watershed. Rainfall data for several other events during the study period were unavailable due to electric power outages or computer failure at the radar.

METHODOLOGY

Hydrologic model

HYMO (**HY**drologic **MO**del) was developed by the Agricultural Research Service of the United States Department of Agriculture in cooperation with the Texas A&M University (Williams and Hann 1973). It is a deterministic, lumped parameter, event-oriented model. The HYMO model was selected for this study because of its ease of use, minimal data requirements, and availability in IBM compatible format.

Hydrograph generation by HYMO is based on the United States Soil Conservation Service (SCS) triangular hydrograph approach, and is accomplished through a series of subroutines. Each subroutine relates to a specific hydrologic command, for example, to create a rating curve from channel geometry, or to compute, route, and add hydrographs.

Table II. Summary of the storm events studied

Event Date	Rainfall duration (h)	Tipping-bucket gauge total (mm)	Five day antecedent rainfall (mm)	Baseflow (m^3/s)	Observed peak flow (m^3/s)
86/07/26	7	44.6	0.0	0.039	1.18
86/09/29	10	43.4	2.0	0.089	2.33
87/05/22	17	31.6	0.0	0.067	0.59
87/07/24	37	46.0	4.6	0.055	0.43
87/09/12	47	64.0	26.2	0.051	0.35
87/10/27	53	33.4	18.4	0.081	0.38

The watershed was divided into eight sub-basins, or reaches (Fig. 2), to permit the use of spatially variable radar rainfall measurements in the HYMO data set. Boundaries of sub-basins were established on the basis of natural and man-made divisions, such as tributaries, roads and culverts.

Using the SCS curve number (CN) procedure, HYMO computed runoff from each sub-basin, starting at the most upstream. The runoff from each sub-basin was routed through the adjacent downstream channel segments using the Variable Storage Coefficient (VSC) flood routing method. Runoff from the lower sub-basin was added to the routed channel flow. This process was repeated by the model until the hydrograph at the watershed outlet was produced.

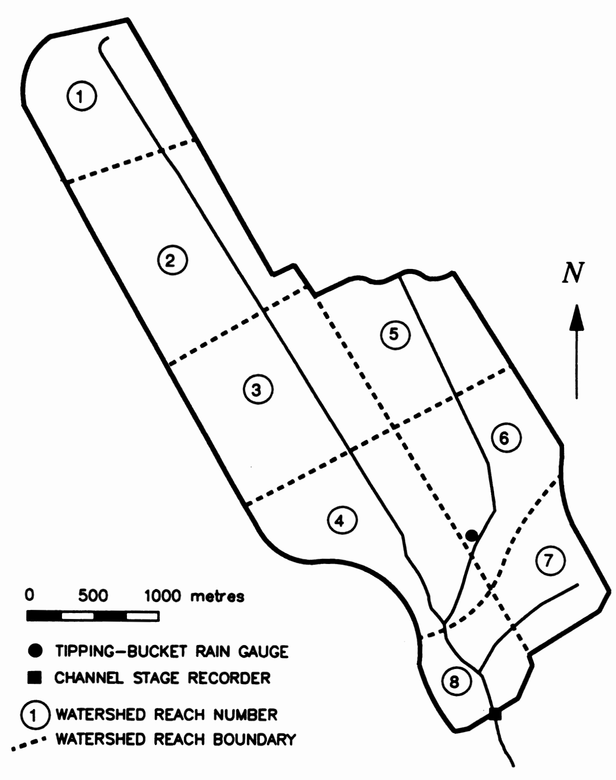

Fig. 2. Map of the St. Dominique watershed showing division into reaches for modelling with HYMO.

SCS curve number

The SCS curve number is a numeric representation of the runoff potential of a catchment. The higher the CN value, the greater the potential for runoff. The CN procedure, and its shortcomings in some cases, has been well documented (SCS 1972; Rawls and Brakensiek 1986; Madramootoo and Enright 1988). The CN is primarily a soils and land use parameter, and does not account for rainfall intensity or duration.

Weighted average values of CN for the watershed were obtained by correlating the soils and land-use information shown in Table I with the guidelines in the SCS (1972) manual. The weighted average watershed curve numbers were 54, 72.4 and 86 for antecedent moisture conditions (AMC) I, II and III respectively.

The CN value corresponding to AMC I was insufficient to generate runoff with HYMO for any of the storm events studied. A CN of 72.4 was used for all but the September 29, 1986 storm. For the latter, a CN value of 86 was required to achieve a reasonably good simulation.

McGill radar

The radar measured rainfall data for this study were provided by the McGill Radar Weather Observatory, located at the western tip of the island of Montreal, at Ste. Anne de Bellevue, PQ. The coordinates of the radar are 45°25'28"N, 73°56'15"W. Marshall and Ballantyne (1975) have published detailed technical information about this S-band (10.4 cm wavelength) radar unit.

The effective range of the McGill radar is a circular area of approximately 200 km radius, centered at the radar. The land surface is fairly flat between the radar and the study area, and for a considerable distance beyond. Thus, range reduction due to background echos from hilly terrain was not a problem.

Battan (1973) described the process of measuring rainfall by radar. Bellon and Austin (1978) have demonstrated that the McGill radar can accurately measure rainfall intensities and rainfall depth accumulations.

It is standard procedure at the McGill radar to archive radar data on magnetic tape. However, both archived and real-time rainfall data were used in this research.

Archived radar data were available for storms dating back to 1978. A computer program available at the radar converted the archived radar data into 10 minute rainfall accumulations for 10 distinct 1 km^2 cells. The location of the cells with respect to the St. Dominique watershed is shown on Fig. 3.

From June 1987 onwards, continuous real-time rainfall data were directed to an IBM PC computer located at the McGill radar. Radar data were obtained from an area comprising 68 bins. Each bin measured 1 km in length by approximately 0.35 km in width. The width of a bin corresponds to a horizontal rotation of one degree by the radar antenna, which is approximately equal to the antenna beam width (0.89°). The area represented by the array of bins encompassed most of the St. Dominique watershed (Fig. 4).

Computer programs were written to store on disk all incoming real-time radar data showing evidence of precipitation, and to convert the data into 5 or 10 minute rainfall accumulations (Schell 1990).

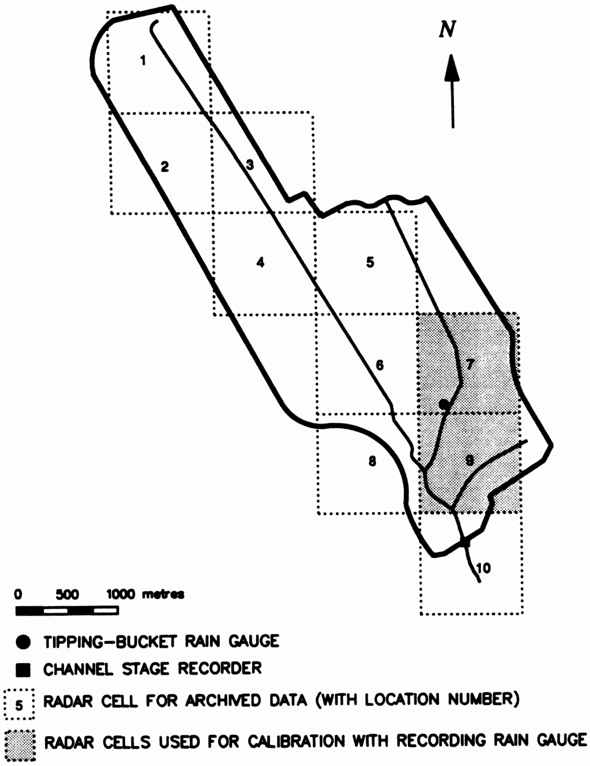

Fig. 3. Map of the St. Dominique watershed showing the ten cells for which archived radar measured rainfall accumulations were obtained.

Converting radar reflectivity data into rainfall intensity

The standard formula for converting radar reflectivity to rainfall intensity is based on an empirical study by Marshall and Palmer (1948). It is known as the Z-R relationship, and for stratiform rain is expressed as:

$$Z = 200\,R^{1.6} \tag{1}$$

where:

Z = radar reflectivity factor (mm^6/m^3), and
R = rainfall rate (mm/h).

Values of the coefficient and exponent in this equation, 200 and 1.6 respectively, depend on both rainfall type and geographic region (Battan 1973; Collier 1987). However, this study used only the original Marshall-Palmer Z-R relationship, as is common practice at the McGill radar.

Since the IBM PC received values of *dBZ* (or $10 \log_{10} Z$) rather than Z, Eq. 1 was transformed as:

$$10 \log_{10} Z = 10 \log_{10} 200 + 16 \log_{10} R \tag{2}$$

Solving Eq. 2 for R yields:

$$R = \text{antilog}_{10}\left[\frac{\text{dBZ} - 23.01}{16}\right] \tag{3}$$

Compensation for a digitizer sensitivity factor resulted in a minor change in Eq. 3 to:

$$R = \text{antilog}_{10}\left[\frac{\text{dBZ} - 12}{16}\right] \tag{4}$$

Using Eq. 4, radar data were converted into rainfall intensities in mm/h for the array of bins over the watershed.

The radar does not provide temporally continuous rainfall data but rather a time-series of "snapshots", each of which was assumed to represent the rainfall intensity for the subsequent period of time until the next "snapshot" or scan was received. The interval was five minutes for real-time data received directly from the radar digitizer, and ten minutes for archived data. Consecutive pairs of real-time data were averaged to ten minute intervals to be consistent with the archived data.

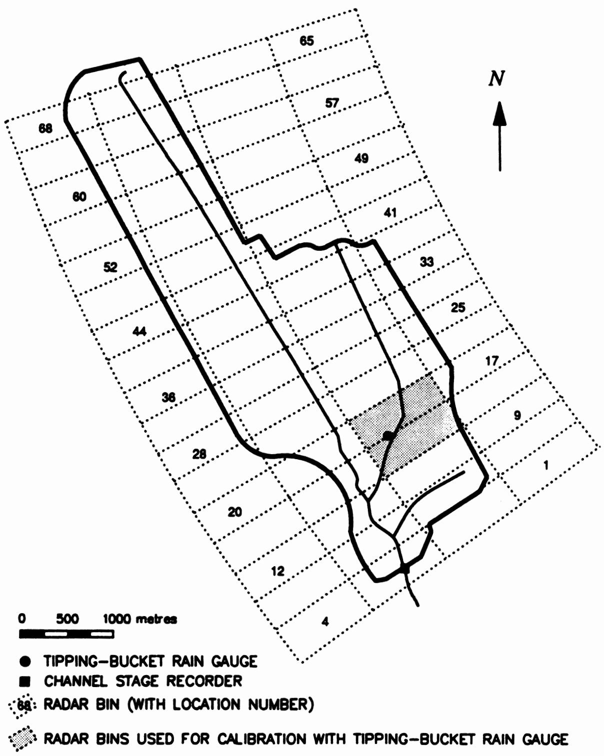

Fig. 4. Map of the St. Dominique watershed showing the 68 bins for which real-time radar measured rainfall accumulations were obtained.

Calibration of radar measured rainfall

While the radar can detect qualitative differences in rainfall intensities over a large area with reasonable accuracy, its measurements were assumed to be less accurate at a single point than those from a raingauge. Since this study sought to examine the effect of using spatially variable versus single point rainfall measurements on the predicted hydrographs, the radar measured rainfall estimates were calibrated with the tipping-bucket raingauge. It was assumed that the latter represented the ground truth value.

Radar rainfall measurements were scaled by the ratio of the total storm accumulation at the raingauge (G) to the average total storm accumulation (R) of the two radar cells nearest the recording raingauge. The same scaling factor, (G/R), was used for the array of cells, for the duration of the storm. Gauge and radar measured rainfall accumulations, the percent difference between them, and the scaling factors are presented in Table III.

For the archived radar rainfall measurements, calibration was based on the average total accumulation of the two cells located nearest the recording raingauge (Fig. 3). Real-time radar data were calibrated using the average of the accumulations from the two 1 km x 0.35 km cells nearest the raingauge (Fig. 4).

Table III. Tipping-bucket raingauge (G) and uncalibrated radar (R) measured accumulations, percent difference between gauge and radar measured rainfall and, the ratio (G/R) of gauge to radar measured rainfall.

Event Date	Tipping-bucket rainfall (mm)	Radar* rainfall (mm)	Percent difference**	G/R
86/07/26	44.6	48.0	7.6	0.93
86/09/29	43.4	28.3	34.8	1.53
87/05/22	31.6	24.9	21.2	1.27
87/07/24	46.0	47.1	2.4	0.98
87/09/12	64.0	49.6	22.5	1.29
87/10/27	33.4	23.1	30.8	1.45

* Measured over tipping-buciet gauge site

** Percent difference = 100 x | (R-G) | /G.

Use of radar measured rainfall in the hydrologic model

The watershed sub-basins as shown on Fig. 2 were larger in area than the individual cells or bins (Figs. 3 and 4) for which radar measured rainfall data were available. When running HYMO with radar measured rainfall data, the rainfall quantity for each sub-basin was estimated by taking the average rainfall accumulation from all of the cells or bins that overlapped the area occupied by that sub-basin.

A summary of the radar measured rainfall totals which were input to each of the sub-basins for simulations of the six rainfall events is presented in Table IV. Also shown are the average rainfall accumulation for the entire watershed, the standard deviation for radar rainfall accumulations over the 8 sub-basins, the maximum difference between the highest and lowest radar rainfall measurement and the raingauge accumulation for each storm.

RESULTS AND DISCUSSION

Rainfall variability

For both the July 26, 1986 and October 27, 1987 storms, rainfall was fairly uniform over the watershed (Table IV). Both storms had a maximum difference of 5.0 mm in the radar measured rainfall accumulation recorded in different reaches of the watershed. The radar measurements indicated that rainfall was variable over the watershed for the other four storms. Maximum differences ranged from 14.2 mm on the July 24, 1987 storm to 19.4 mm on the September 12, 1987 storm.

Coefficient of efficiency

The coefficient of efficiency (R^2) was introduced by Nash and Sutcliffe (1970) as an objective means to describe the degree of association between observed and estimated streamflows. It is obtained through linear regression analysis by:

$$R^2 = (F_o^2 - F^2)/F_o^2 \tag{5}$$

where R^2 is the dimensionless coefficient of efficiency. The "index of disagreement", F^2, is defined by:

Table IV. Calibrated radar rainfall accumulations (mm) averaged over the eight watershed sub-basins

Watershed reach number	Calibrated radar measured rainfall (mm) 86/07/26	86/09/29	87/05/22	87/07/24	87/09/12	87/10/27
1	42.6	29.3	34.8	36.3	53.9	34.5
2	45.2	33.7	40.0	40.8	53.5	34.0
3	47.6	38.0	41.7	50.5	59.1	33.3
4	45.9	42.4	30.7	46.4	51.9	34.0
5	47.2	39.6	38.8	44.7	63.7	32.2
6	44.6	43.4	31.6	48.8	58.5	31.0
7	43.2	45.5	27.0	49.3	54.8	29.5
8	43.5	45.0	24.9	39.9	44.3	33.2
Average	45.0	39.6	33.7	44.6	55.0	32.7
Standard Deviation	1.9	5.7	6.2	5.1	5.8	1.7
Maximum Difference	5.0	16.2	16.8	14.2	19.4	5.0
Gauge Total	44.6	43.4	31.6	46.0	64.0	33.4

$$F^2 = \Sigma(q' - q)^2 \tag{6}$$

where q and q' are the observed and computed discharges at corresponding times. The "initial variance", F_o^2, is defined by:

$$F_o^2 = \Sigma(q - q_{avg})^2 \tag{7}$$

where q_{avg} is the mean of the observed discharges.

A value of R^2 close to one indicates good agreement between the observed and predicted hydrographs, while a low R^2 denotes a poor quality simulation.

A listing of the computed values of R^2 for each of the storm hydrographs is presented in Table V, along with a summary of the observed and predicted hydrologic parameters. The list of R^2 values indicates that only the July 26, 1986 and September 29, 1986 storm hydrographs were accurately simulated. In both cases, more accurate simulations were obtained with the radar rainfall data than the single raingauge measurement.

The radar predicted hydrograph for the May 22, 1987 storm resulted in a positive but low value of R^2. The gauge predicted hydrograph for the same storm event resulted in a negative R^2 value. For the final three storms, both the radar and raingauge simulations resulted in negative values of R^2.

The simulations that resulted in negative values of R^2 indicate the need for further refinements in the calibration of the model.

Simulated hydrographs

The observed and predicted hydrographs for four of the six storm events were plotted together with the gauge and radar derived hourly rainfall accumulations (Figs. 5 to 8). Storm hydrographs for the July 24, 1987 and September 12, 1987 events were omitted. For these two storms, neither radar nor raingauge rainfall measurements resulted in simulated hydrographs worthy of presentation.

The displayed values of radar measured rainfall are the average hourly total from the same pair of radar cells used for calibration. The HYMO input data files for simulations that used radar data were supplied with separate 10 minute rainfall accumulations for each of the eight reaches. Total accumula-

Table V. Peak flow rate, Q_p (m^3/s) and runoff depth D (mm) predicted by HYMO using raingauge and radar measured rainfall, and the computed values of the coefficient of efficiency R^2 for discharges predicted by HYMO

Event date	Observed catchment response: Baseflow (m^3/s)	Q_p (m^3/s)	D (mm)	Predicted using gauge measured rainfall: Q_p (m^3/s)	D (mm)	R^2	Predicted using radar measured rainfall: Q_p (m^3/s)	D (mm)	R^2
86/07/26	0.039	1.18	6.49	1.20	4.78	0.821	1.21	4.99	0.921
86/09/29	0.089	2.33	16.72	3.89	14.86	0.530	3.04	12.09	0.692
87/05/22	0.067	0.59	4.16	0.33	1.18	-0.187	0.47	2.00	0.366
87/07/24	0.055	0.43	2.69	0.81	4.66	-3.893	0.90	4.30	-5.397
87/09/12	0.051	0.35	2.81	1.41	10.70	-39.456	0.72	8.14	-11.574
87/10/27	0.081	0.38	3.23	0.23	0.93	-0.603	0.33	1.52	-0.280

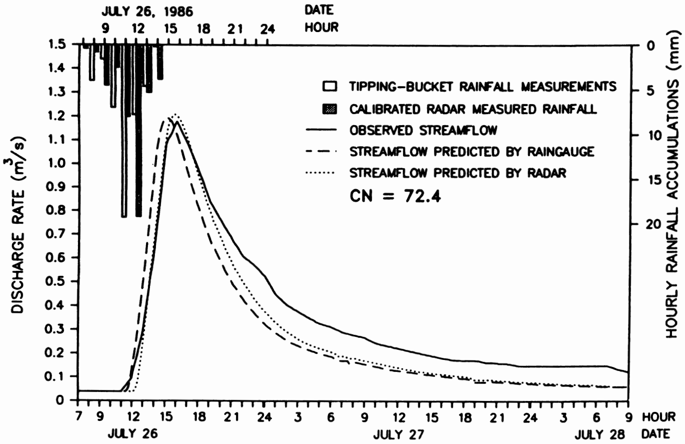

Fig. 5. Predicted and observed streamflows for the storm of July 26, 1986.

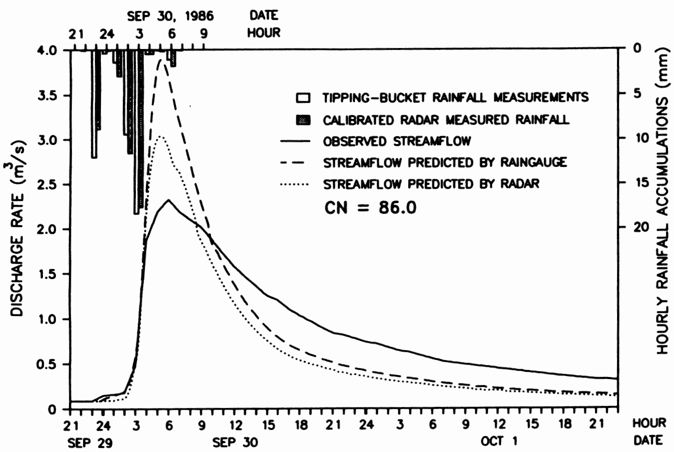

Fig. 6. Predicted and observed streamflows for the storm of September 30, 1986.

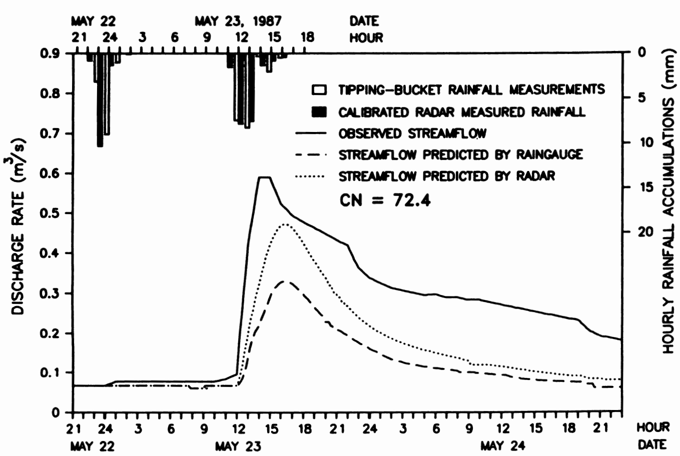

Fig. 7. Predicted and observed streamflows for the storm of May 22-23, 1987.

tions for each reach are shown in Table IV.

Simulations of the July 26, 1986 and September 29, 1986 events (Figs. 5 and 6) produced good results with both radar and gauge measured rainfall. For the May 22, 1987 (Fig. 7) and

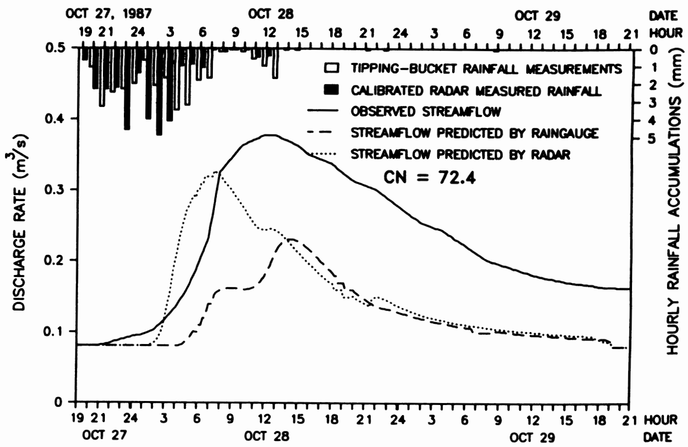

Fig. 8. Predicted and observed streamflows for the storm of October 27-28, 1987.

October 27, 1987 (Fig. 8) storms, the hydrographs generated using radar and gauge measured rainfall differed considerably from the observed hydrograph.

Rainfall pattern, intensity and duration appeared to be significant factors affecting simulation accuracy, regardless of the rainfall data source. Storms of short duration (less than 12 hours), and high intensity, such as those of July 26, 1986 and September 29, 1986, were more accurately simulated by HYMO than prolonged, low intensity rainfall events using both rainfall sources.

Time to peak flow, T_P, is defined as the time between the first detected rise in streamflow and the peak streamflow. On the first two storm hydrographs (Figs. 5 and 6), the predicted T_P from both the radar and gauge generated hydrographs was within one hour of the observed.

For the May 22, 1987 storm (Fig. 7), the times to peak flow of the hydrographs predicted using both radar and gauge measured rainfall were 2.3 hours later than what was observed. Simulations of the October 27, 1987 event (Fig. 8) resulted in a predicted T_P that was 4.5 hours early using radar measured rainfall and 2.2 hours late using gauge measured rainfall. This discrepancy in the predicted T_P values is an indication that, for prolonged storms (more than 12 hours), the radar calibration factor (G/R) should be calculated hourly, rather than on the basis of total storm accumulation. This approach would more accurately reflect the changing nature of the rainfall intensity and rain drop size during the course of the storm.

Peak flows

Table V summarizes the observed and predicted peak flowrates, Q_P, and the runoff depths, D, for the six events studied. Also listed are the computed values of the coefficient of efficiency.

Of the six rainfall events, it appears that those with observed peak flows greater than 0.6 m^3/s were better simulated. The storm events of July 26, 1986, September 29, 1986 and May 22, 1987 had observed peak discharge rates of 1.18, 2.33 and 0.59 m^3/s, respectively and the simulated results were reasonably accurate. Conversely, the July 24, 1987, September 12, 1987 and October 27, 1987 storm events had peak flowrates of only 0.43, 0.35 and 0.38 m^3/s, respectively, and were not well simulated by the model. The apparent relationship between peak flow magnitude and simulation accuracy may indicate that the streamflow rating curve was more reliable at higher flow rates. Another possibility is that, at higher discharges, stream velocity was less affected by vegetation and other obstructions in the channel.

The predicted peak flow for the July 26, 1986 event was closest to the observed. Both gauge and radar predicted rainfall inputs resulted in estimated peak flows within 2.5% of the observed.

Predictions of peak flow for the September 29, 1987 and May 22, 1987 storms were more accurate with radar than gauge measured rainfall. During both storms, the radar detected a high degree of spatial variability in rainfall accumulations.

The list of rainfall values (Table IV) for the September 29 storm reveals that the southern part of the watershed, where the raingauge was located, received up to 16.2 mm more rainfall than the north. Since the raingauge simulation used the gauge measurement for all eight reaches, the peak flowrate was overestimated.

Table IV indicates that, on May 22, 1987, the radar detected 10.1 mm more rainfall over the central portion of the watershed than in the vicinity of the recording raingauge and 16.8 mm more than in the extreme southern portion of the watershed. The effect of areal rainfall variability on streamflow may have been responsible for the "bump" in the observed hydrograph occurring at 2200 hours on May 23, 1987 (Fig. 7). However, it appears that HYMO is not sensitive to this rainfall input, since the "bump" did not appear in the hydrograph predicted using radar rainfall data.

Runoff depth

For all six storms, simulations using both radar and raingauge measurements resulted in poor estimates of runoff depth. In the four storms for which hydrographs were presented, the observed runoff depth exceeded predicted values. A major contributing factor to this trend was the falling limb of the hydrograph. After peak flow was attained, the predicted hydrographs declined more rapidly than the observed hydrographs.

Difficulties in accurately simulating the falling limb of hydrographs are common when using the CN method, since it does not account for depression storage or subsurface drainage. Other methods, such as that developed by Green and Ampt (Green and Ampt 1911), allow the user to adjust the depression storage input and could help to improve the accuracy of simulated hydrographs.

CONCLUSIONS

Radar measured rainfall data for six rainfall events were obtained from the McGill weather radar and calibrated with measurements from a single tipping-bucket raingauge. The rainfall data were subsequently used in a hydrologic modelling study of an 8.13 km^2 agricultural watershed in south-western Quebec. Based on the work conducted in this study, the following conclusions were made.

1. Radar measured rainfall rates for selected regions within the effective range of the McGill radar can be obtained directly from the VAX computer system at the radar building, and rapidly transferred into an IBM PC.
2. Rainfall measured by the McGill weather radar can be input directly into HYMO and used to generate streamflow hydrographs.
3. For high intensity, short duration, convective rainstorms, the HYMO model can produce a simulated hydrograph closely resembling the observed using either recording raingauge or calibrated radar measured rainfall.
4. For long duration, low intensity rainfall events, the HYMO model does not accurately simulate storm hydrographs with either raingauge or radar measured rainfall input.
5. For high intensity, short duration storm events, where rainfall is spatially variable over the watershed, it appears that calibrated radar rainfall measurements can provide rainfall inputs to a rainfall-runoff model that are superior to those obtained from a single raingauge. Based on the two storm events that exhibited the above characteristics, rainfall inputs from the radar can generate a more accurate predicted hydrograph than when the rainfall input is obtained from a single raingauge.

ACKNOWLEDGMENTS

The financial support of the McGill Weather Radar Observatory, the Conseil des Recherches en Agriculture et Pêcheres et Alimentation du Quebéc, and the Fonds pour la Formation de Chercheurs et L'Aide a La Recherche is greatly appreciated.

REFERENCES

Battan, L.J. 1973. *Radar Observation of the Atmosphere.* Chicago, IL: University of Chicago Press.

Bellon, A and G.L. Austin. 1978. The evaluation of two years of real-time operation of a short-term precipitation forecasting procedure (SHARP). *Journal of Applied Meteorology* 17(12):1778-1787.

Collier, C.G. 1987. Accuracy of real-time radar measurements. In *Weather Radar and Flood Forecasting*, eds. V.K. Collinge and C. Kirby, 71-95. Chirchester, England: John Wiley and Sons.

Enright, P. and C.A. Madramootoo. 1988. A comparison between the curve number method and the Green-Ampt equation for predicting excess rainfall in Quebec. ASAE Paper No. NAR-88-403. St. Joseph, MI: ASAE.

Green, W.H. and G.A. Ampt. 1911. Studies on soil physics. Part 1 - The flow of air and water through soils. *Journal of Agricultural Science* 4(1):1-24.

Madramootoo, C.A. and P. Enright. 1988. Applicability of the soil conservation service equations for runoff prediction in the Ottawa-St. Lawrence lowlands. *Canadian Journal of Civil Engineering* 15(5):759-765.

Madramootoo, C.A., P. Enright, V.T.V. Nguyen, R.S. Broughton and S.O. Prasher. 1988. Impact of the July 14, 1987 rainstorm on agricultural runoff in western Quebec. *Canadian Water Resources Journal* 13(2):18-26.

Marshall, J.S. and E.H. Ballantyne. 1975. Weather surveillance radar. *Journal of Applied Meteorology* 14(7):1317-1338.

Marshall, J.S. and W.M. Palmer. 1948. The distribution of raindrops with size. *Journal of Meteorology* 5(4):165-166.

Nash, J.E. and J.V. Sutcliffe. 1970 River flow forecasting through conceptual models, 1. A discussion of principles. *Journal of Hydrology (Netherlands)* 10:282-290.

Rawls, W.J. and D.L. Brakensiek. 1986. Comparison between Green-Ampt and curve number runoff predictions. *Transactions of the ASAE* 29(6):1597-1599.

Schell, G.S. 1990. The application of radar measured rainfall to hydrologic modelling. Unpublished M.Sc. thesis, Department of Agricultural Engineering, McGill University, Montreal, PQ.

SCS. 1972. Hydrology. In *National Engineering Handbook*, Section 4. Washington, DC: Soil Conservation Service.

Williams, J.R. and R.W. Hann Jr. 1973. *HYMO: Problem-oriented computer language for hydrologic modeling*. Users Manual. College Station, TX: Agricultural Research Service, USDA, and Texas Agricultural Experiment Station, Texas A & M University.